Arch. Metall. Mater. **68** (2023), 1, 57-70

DOI: https://doi.org/10.24425/amm.2023.141473

S. ŻAK[1*], D. WOŹNIAK[2]

CONTROLLING THE STATE OF RESIDUAL STRESSES IN RAILWAY RAILS BY MODIFYING PASS DESIGN OF STRAIGHTENING ROLLERS

The paper presents a summary of research on the possibility of influencing the state of residual stresses in railway rails by changing the pass design of vertical and horizontal straightener rollers and optimising their distribution on the rail perimeter. The presented results are devoted to the influence of profiled rollers on the level of residual stresses. A wide range of theoretical considerations were carried out based on the use of the finite element method using the commercial Forge software package. In order to verify the results of the theoretical considerations most reliably, a series of "in situ" experiments were conducted in industrial conditions on an existing production line. The tests were carried out on 120 meters long 60E1 railway rails. A significant reduction in the level of residual stresses compared to the standard requirements was achieved.

Keywords: railway rail; residual stresses; straightening process; straightening rollers; strain gauge method

1. Introduction

Modern rail transport, especially at high speeds, places high demands on the quality of tracks, the most important element of which is the rail, which plays the dual role of both a support and a guide in the track. Modern rails must be characterised by a high level of mechanical properties, including brittle cracking resistance, fatigue strength, fatigue crack growth rate, as well as appropriate geometrical features, primarily low dimensional deviations and straightness along the entire length of the rails [1]. The European standard EN 13674-1 [2] allows a maximum straightness deviation in the vertical plane of 0.3 mm over a measuring length of 3 m. Those special requirements in terms of straightness result from the necessity to reduce the vibration amplitude in the vertical plane of the rail during track operation. Too large deviations from straightness may initiate vibrations leading not only to a reduction in ride comfort, but also to damage to rail vehicles and tracks. After rolling and cooling, the rails do not meet the specified straightness parameters, therefore the required value of straightness of the rails is obtained by straightening using roller straighteners. The greatest residual stresses are introduced into the finished product during this process.

Most of the standards and specifications of railway companies [2-6] include the necessity to measure residual stresses of the rail and their maximum allowable level is set not only at one point, but often also at precisely defined locations around the perimeter of the rail. In accordance with the European standard EN13674-1 [2], stress measurement is performed in the axis of the rail foot, and the maximum allowable value cannot exceed 250 MPa for all types of rails and rail steel grades produced. The high criteria set by railway companies for stresses in rails result from the overlapping of residual stresses with quasi-static thermal stresses and dynamic stresses from operation, which may lead to the formation of cracks starting from single surface material discontinuities or subsurface microcracks located in rail head or foot. In a finished rail, after successive production stages, i.e. rolling, cooling and straightening, the following characteristic distribution of stresses is determined: tensile stresses occur in the head, which then change their character into compressive stresses, reaching the highest value in the neutral axis of the web and reverting into tensile stresses in the foot area. After a certain period of operation, as a result of crushing the surface layer, tensile stresses in the rail head change their character and transform into compressive stresses, but only to a depth of about 7-10 mm [7]; tensile stresses occur in the rest of the head, while the state of stress in the rail foot remains constant throughout its operation. By lowering the level of residual stresses in the rail foot, the critical depth of the crack originating in this area is also

[1] ARCELORMITTAL POLAND S.A., AL. JÓZEFA PIŁSUDSKIEGO 92, 41-300 DĄBROWA GÓRNICZA, POLAND
[2] INSTITUTE FOR FERROUS METALLURGY, UL. KAROLA MIARKI 12, 44-100 GLIWICE, POLAND
* Corresponding author: sylwester.zak@arcelormittal.com

deepened. Moreover, the reduced level of residual stresses results in a reduction of the mean value of operational stresses, as a result of which slows down the crack development. Additionally, rolling contact fatigue defects such as shelling, head checking, squat and other types can develop in the rail head, which often leads to a fracture in the rail. To counteract the development of these defects, it is desirable to keep tensile stress in this part of the rail as low as possible. If tensile stresses reach the critical value of the fracture toughness factor K_{Ic} (determining brittle cracking resistance), the crack develops in an uncontrolled manner, leading to a fracture in the rail.

The level of residual stresses translates into the operational durability and reliability of rails, which are the most expensive component of railway routes, and thus affect the economic results of railway companies, but above all, it has a direct impact on the safety of railway traffic. The total value of residual, operational and thermal stresses cumulated in the rail may lead to the loss of track stiffness and its buckling. Buckling of the track occurs as a result of the stress release and is combined with overcoming the resistance of ballast and the track frame stiffness – an example illustration of this phenomenon is shown in Fig. 1. In extreme cases, the cumulated stresses may lead to the formation of a rail fracture, as was the case in the railway disaster in Hatfield, UK, about 50 km north of London, where a train at a speed of about 185 km/h derailed. The locomotive and the first two cars remained on the rails in an upright position; all subsequent cars derailed, and the train was split into three parts. The dining car, which was the eighth in the set, overturned on its side and stuck into the poles of the traction line, as a result of which it was practically crushed. The entire accident happened 17 seconds after the rail broke – see Fig. 2. The rail cracking was associated with the co-occurring small surface cracks resulting from the development of rolling contact fatigue defects, mainly of the head checking type.

Fig. 1. Contactless track buckling [8]

The technological process of cooling rails is the stage in the production of rails, where the level of residual stress is already introduced into the product, it arises as a result of temperature differences between the rail head, web and foot. Temperature differences are related to a different weight distribution on the rail cross-section, e.g. for the 60E1 profile, the head is 40.75%

Fig. 2. Train accident in Hatfield, Great Britain [9]

of the total rail weight, the web 22.02% and the foot 37.23% respectively, and the shape of these elements, and thus the amount of cumulated thermal energy resulting in the delayed onset of the phase changes occurring first on those parts of the rail that have the lowest temperature. The literature data [10] shows that the rail after cooling, and before straightening, has relatively low residual stresses varying along its height in the range from about -50 MPa in the rail web to about +50 MPa in the rail head and foot. These values partially coincide with the authors' own experiments, during which the measurements of the residual stresses for rails after cooling without and with initial bending using the cutting method for the entire range of curvatures occurring after cooling were performed $R = 73{,}5$ m to $R = 3330$ m. Residual stresses were determined in the foot axis, on both sides of the web in the neutral axis and on the running surface in the head axis. The residual stresses in the rail foot after cooling were tensile and the values ranged from 95 to 120 MPa, in the web compressive and the values ranged from –5 to –55 MPa, and rather compressive from -30 to 2 MPa in the head. Compared the authors' results to the work [10], where the following distribution of residual stresses is given after cooling the rails: in the head from 30 to 55 MPa, in the web from –40 to –50 MPa, and in the foot from 30 to 50 MPa, the obtained measurements showed an identical character and a similar range of stresses in the rail web, while in the rail foot, an increased value of tensile stresses was observed with a simultaneous decrease in their value in the rail head. The differences in the residual stress distribution in the discussed examples could result from unequal cooling conditions of the rails, the use of different bending values in the cooling beds or the length of the tested rails. As a result of the plastic deformation of the rail, during the straightening process, stresses are introduced into the rail that overlap with the residual stresses after cooling, and this is the technological stage of rail production that introduces the highest stresses into the product. After straightening, high tensile stresses appear in the head and foot of the rail, which decrease towards the center of the rail and transform into compressive stress in the web. By using appropriate straightening technologies, rail manufacturers are able to keep the residual stress in the rail foot below the permissible

value of 250 MPa of standard EN13674-1:2011+A1:2017 [2]. To maintain a low level of residual stresses, it is essential to use 9-roller straighteners with a variable distance between rollers in a wide range of values, which can significantly reduce the level of residual stresses in the rail. For a given distance between the rollers, there are many sets of setting values which result in a straight rail. With appropriately optimized settings, it is possible to reduce the level of residual stresses in the rails, which has been confirmed both by numerical simulations and tests in industrial conditions [10-18]. Literature analysis did not reveal any publications devoted to the research on changing the pass design of straightener rolls to the residual stress level. The own research on the influence of changes in the shape of the straightening rollers and various combinations of their settings, discussed in this paper, proved their significant influence on the reduction of residual stresses in rails after straightening operation.

2. The concept and scope of study

The discussed results of the work on reducing residual stress in the rail foot are a summary of three stages of research on the impact of pass design of straightener rollers to the stress level [19-21] and were carried out as part of the project co-financed by the National Centre for Research and Development Poland entitled "Innovative and safe rails with a low level of residual stresses in the foot of the rail" – POIR.01.02.00-00-0167/16. The studies were carried out in the following scope:

– development of a new pass design of vertical and horizontal straightener rollers,
– development of a research programme including three variants of the roller system in a set of straighteners,
– numerical simulations of the straightening process for individual variants of the straightening roller system,
– conducting tests in industrial conditions in a vertical and horizontal straightening machine of a heavy section mill at ArcelorMittal Poland S.A. for the assumed variants of the straightening rollers installation,
– carrying out measurement of residual stresses in rails after straightening, carrying out mechanical tests and evaluation of geometric parameters, shape and straightness of the rail.

The above theoretical assumptions were reflected in the development of technical documentation for pass design of the straightening rollers. They were then fully applied to industrial research.

2.1. Pass design of straightening rollers

The following theoretical assumptions were adopted when developing a new, innovative pass design of vertical and horizontal straightener rollers, which were aimed at:

– modifying the shape of the rollers resulting in a reduction of the roller – strand contact stresses and the distribution of these stresses,
– reducing the growth of residual stress in the area of the rail head,
– obtaining the smallest possible strain necessary to straighten the strand,
– reducing the size of the contact surface of the roller and the straightened rail.

The adopted criteria are conditioned by the slight possibility of changing the shape of the head rollers of the vertical straightener, adjusted to the rail head profile. A new method of pass design of vertical straightener foot rollers in two variants characterised by a different shape of the roller-rail contact surface and a new pass design method for horizontal straightener rollers varied by the size of the flange were developed.

2.2. Plastometric tests

In order to develop a mathematical description of the material flow curve during cold strain, plastometric tests were carried out, in which Ø10×12 mm samples were deformed at different strain rates and at different temperatures. A diagram of the strain of a cylindrical sample in a Gleeble simulator is shown in Fig. 3. As part of this study, it was necessary to determine the flow curve for the cold strain conditions and to determine the yield strength of the deformed material in the temperature range corresponding to the cooling of the material after rolling.

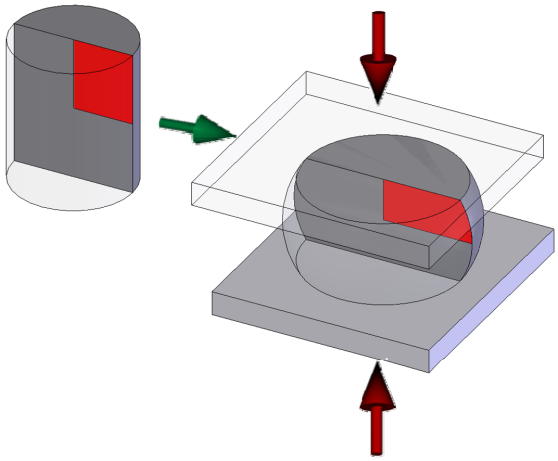

Fig. 3. Strain of a rolled sample along with the marked part of a sample set due to the symmetry in numeric calculations

During plastometric tests, the software controlling the Gleeble 3800 simulator saves the test results in tabular form, in which it calculates the stress from the measured force in accordance with the engineering method:

$$\sigma_e = \frac{F_m}{S} \tag{1}$$

where:

σ_e – the value of stress from the measured force,
F_m – the value of the force from the measurement,
S – the current mean cross-section.

However, this approach does not take into account the influence of friction and the inhomogeneous distribution of the strain velocity and temperature field on the value of the yield stress. The inverse analysis method is used to determine the actual stress-strain curve. In order to determine the actual value of the yield stress, the method of initial inverse analysis uses a numerical simulation of the sample compression process. The sample deformation is divided into 100 time steps. At each time step, the value of yield stress is determined while converging the calculated force to the measured force. In order to take into account the inhomogeneous distribution of the strain rate and temperature in the sample, the formula is used:

$$\sigma = a\sigma_e \left(\frac{\dot{\varepsilon}}{\dot{\varepsilon}_n}\right)^m \exp\left[\frac{Q_{def}}{R}\left(\frac{1}{T}-\frac{1}{T_n}\right)\right] \tag{2}$$

where:

a – correction factor taking into account the friction effect,

$\dot{\varepsilon}$ and T – strain rate and temperature for a given point in the sample,

$\dot{\varepsilon}_n$ and T_n – nominal values of strain rate and temperature (set for the test),

Q_{def} and m – activation energy and strain velocity sensitivity factor.

For each plastometric test, the relationship "actual stress – strain" is determined in tabular form. In order to simulate the rail straightening process, the FORGE program requires a description of the rheology of the material in tabular form or a developed rheological model. The flow curve during cold deformation is most often described by the Hensel-Spittel model in the form:

$$\sigma = A\cdot\exp\left(m_1\cdot T\right)\cdot T^{m_9}\cdot\varepsilon^{m_2}\cdot \exp\left(\frac{m_4}{\varepsilon}\right)\cdot\left(1+\varepsilon\right)^{m_5\cdot T}\exp\left(m_7\cdot\varepsilon\right)\cdot\dot{\varepsilon}^{m_3}\cdot\dot{\varepsilon}^{m_8\cdot T} \tag{3}$$

wherein

$$\begin{cases}\varepsilon = \varepsilon & \text{if} \quad \varepsilon < \varepsilon_{soft} \quad \cup \quad \varepsilon_{soft} = 0\\ \varepsilon = \varepsilon_{soft} & \text{for} \quad \varepsilon \geq \varepsilon_{soft}\end{cases}$$

where:

A, m_1, m_2, m_3, m_4, m_5, m_7, m_8, m_9 – model coefficients,

ε_{soft} – softening strain, above which the stress value remains constant.

Based on the preliminary numerical simulation of vertical straightening of the rail, a set of strain parameters occurring in the straightening process was determined. During the tests, the samples were deformed at 20-100°C at a strain rate of 0.01-10.0 s^{-1}. Stress-strain curves were obtained once the samples were deformed. In the next stage, inverse analysis was used to determine the actual flow curve. The determination of the flow curve in a tabular form allowed for the development of a rheological model. Due to the shape of the obtained curves, an approach was applied in which the stress above strain ε_{soft} is a constant value. Such attitude allowed for a more precise fit of the flow curve model with the coefficients given in Tab. 1.

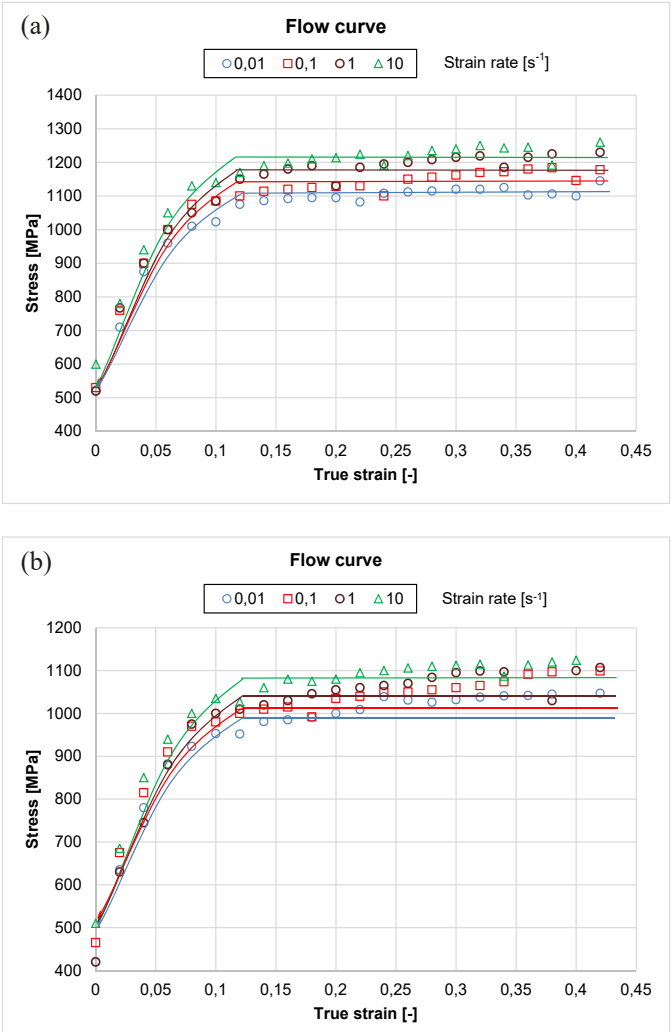

Fig. 4. Comparison of flow curve determined using reverse analysis (line) to the curve calculated with the use of engineering method (symbol) for the strain temperature (a) 20°C and (b) 100°C after adjusting with the coefficients. The value of strain rate is given in the key

TABLE 1

Coefficients of flow curve

A	m_1	m_2	m_3	m_4	m_5	m_7	m_8	m_9	ε_{soft}
2343.23	$-1.399\cdot10^{-3}$	0.2989	$1.322\cdot10^{-2}$	$5.75\cdot10^{-4}$	0	0	0	0	0.11

where:

A, m_1, m_2, m_3, m_4, m_5, m_7, m_8, m_9 – model coefficients,

ε_{soft} – softening strain, above which the stress value remains constant.

2.3. Determination of the material's yield strength

To determine the yield strength of the material during cooling, plastometric tests were performed, in which the samples were first annealed at 1000°C for 30 s, and then cooled at a rate of 1°C/s to a strain temperature in the range of 900-50°C with a strain rate of 0.01 s^{-1}. Fig. 5 shows the stress-strain curves. Then, the actual rheology of the material was determined using preliminary inverse analysis. The obtained curves are shown in Fig. 6. After filtering, the tabular data were entered into the Forge program.

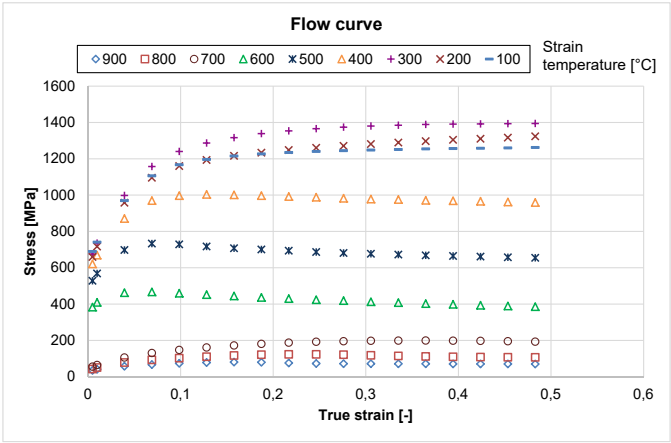

Fig. 5. Determined tension-strain curves with the use of engineering method for the strain rate of 0.01 s^{-1} at a strain temperature given in the key

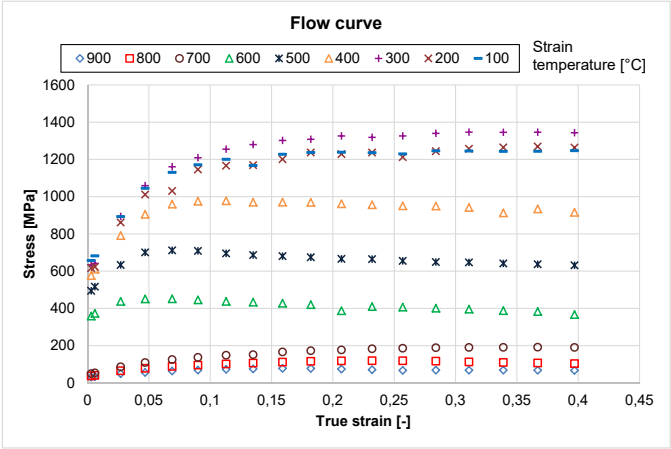

Fig. 6. Comparison of the flow curve determined using reverse analysis (line) to the curve calculated with the use of engineering method (symbol) for the strain rate of 0.01 s^{-1}, the level of strain temperature is given in the key

2.4. Computer simulations of the rail straightening process

The input data for the straightening simulation in both vertical and horizontal straighteners was the state of residual stresses in the rail after cooling it from the rolling end temperature to the temperature enabling the straightening of the rails, i.e. a maximum of 60°C. For this purpose, a numerical simulation of rail cooling from 900°C to ambient temperature (20°C) was performed on the basis of plastometric tests. As a result of uneven cooling of the rail (thicker parts of the rail cool down more slowly), it bends first towards the foot and then towards the head. As a result, tensile stresses arise in the rail foot. The result of the numerical simulation of the rail cooling process is shown in Fig. 7. The material data determined in plastometric

Fig. 7. Distribution of residual stresses after cooling

tests and by calculations in the JMatPro program together with the constructed three-dimensional model of the rail strand and straightener rollers constituted the data for simulation in the commercial program Forge. The numerical simulations of the straightening process included the basic variant with the previously used rollers of both straighteners and three variants of the arrangement of new profiled rollers:

– variant 1 assumed the use of profiled rollers with different concavities on the R3 and R5 shafts of a vertical straightener and rollers on a horizontal straightener with the shape used so far. The schematic arrangement of the shafts in the vertical straightener is shown in Fig. 8, the shaped rollers were mounted in a traverse arrangement on the shafts R3 and R5, they influenced the bottom surface of the rail foot. The shaped roller used on the R5 shaft had an increased concavity by 66% compared to the roller mounted on the R3 shaft. The remaining foot rollers, i.e. those used on the R1 and R7 shafts, had a flat surface.

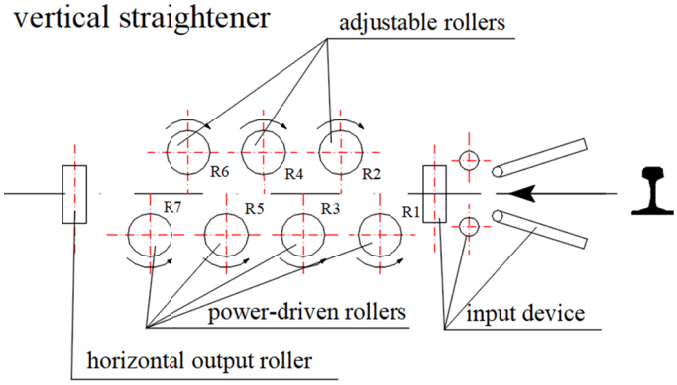

Fig. 8. Schematic representation of the shaft arrangement in a 7 roller vertical straightener

– variant 2 included the same installation of profiled rollers on a vertical straightener as in variant 1 and additionally the use of new rollers with a small flange and without a flange on a horizontal straightener. In this system, on the horizontal straightener, the standard introducing roller on the R1 shaft has been used so far, while on the R2 to R7 shafts, rollers with a small flange reduced by 5 mm compared to the currently used ones were used, while the rollers on the last two shafts, R8 and R9, were equipped with new shaped rollers in whose collar has been completely removed. The arrangement of the individual shafts of the horizontal straightener is shown in Fig. 9.

– variant 3 with the use of profiled rollers with a small concavity on all shafts of the vertical straightener located on the side of the rail foot, i.e. R1, R3, R5 and R7, and the use of rollers with a small flange and without a flange on the horizontal straightener. In this variant, the same foot rollers with a smaller concavity were used on the vertical straightener, i.e. the same as the R3 roller in the first variant of the described tests.

In the numerical simulation of straightening process, it was assumed that the rails before straightening had their residual stress state as determined in the numerical simulation of the cooling process. For the purposes of the straightening simulation, it was assumed that the rail before entering the straightener did not show any significant curvature on the modeled 6 meter section. In the straightening simulation, the rollers were treated as rigid tools – the simulation does not take into account their deformation. During straightening, small plastic deformations of the material occur $\varepsilon = 0.1$, it is simplified that the roller does not deform.

A mesh consisting of 138,000 nodes and 751,000 elements was used to simulate the straightening. The simulations were carried out on a 6 meter section of the rail, the deformed elements were filled with tetrahedral elements (a triangle at the base), and the non-deformed elements with surface elements (triangles). The mesh size was assumed to be 9 mm, and in the areas of contact of the straightening rolls, the density was increased to 5 mm. How many steps was the simulation performed in?

In the straightening simulation, the Treska friction model was used (friction coefficient $\mu = 0.45$; heat exchange coefficient with the environment $h = 10{,}000$ W/K·m^2 and with the tool 20,000 W/K·m^2. The Coulomb friction model was used in the rolling simulation (coefficient of friction $\mu = 0.25$; heat exchange coefficient with the environment $h = 10{,}000$ W/K·m^2 and

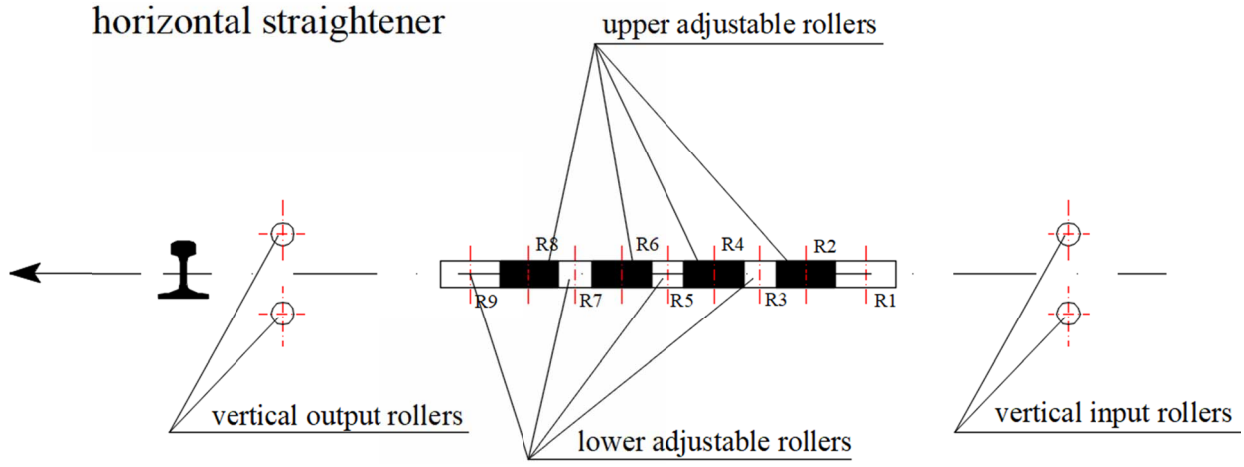

Fig. 9. Schematic representation of the shaft arrangement in a 9 roller horizontal straightener

with the tool 20,000 W/K·m^2. The numerical simulation of the straightening the rail in the vertical straightener was performed in 2603 steps, and the simulation of straightening in the horizontal straightener was performed in 2795 steps.

The results of the simulations carried out were the calculated residual stresses in the individual stages of straightening, i.e. after the rail exited each roller of the vertical and horizontal straightener. To compare the changes in residual stresses in the longitudinal direction, a simulation stage was selected in which the rail was subjected to all straightening rollers simultaneously, and an additional simulation consisting in removing the load was performed for this state of deformation. Fig. 10 shows an example of a selected simulation stage, in which, after unloading, residual stresses were determined on the cross-section after

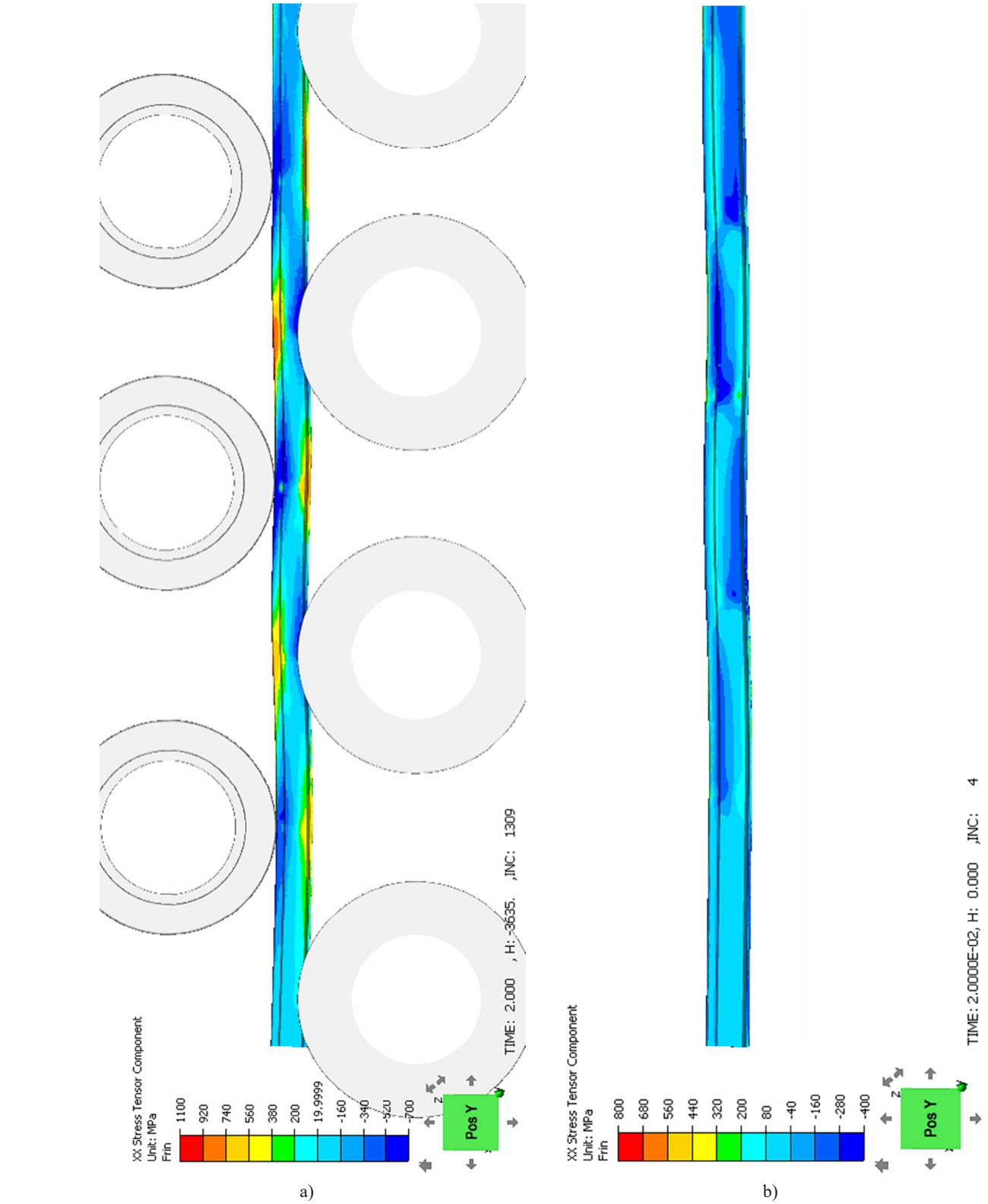

a) b)

Fig. 10. Distribution of residual stresses in the longitudinal direction during straightening a), and after removing the load b), calculated for variant 3

each straightening roller. Fig. 11 shows the distribution of stress components in the vertical and horizontal directions for the cross-section for variant 3 after roller 9 of the horizontal straightener. When analysing the obtained stress distribution, it was found that compressive stresses arise in the rail head for the vertical direction. In the case of the foot, residual stresses were observed in the rolling direction, i.e. perpendicular to the cross-section; for variant 1, the calculated values are compressive, and in the remaining variants, tensile values were obtained.

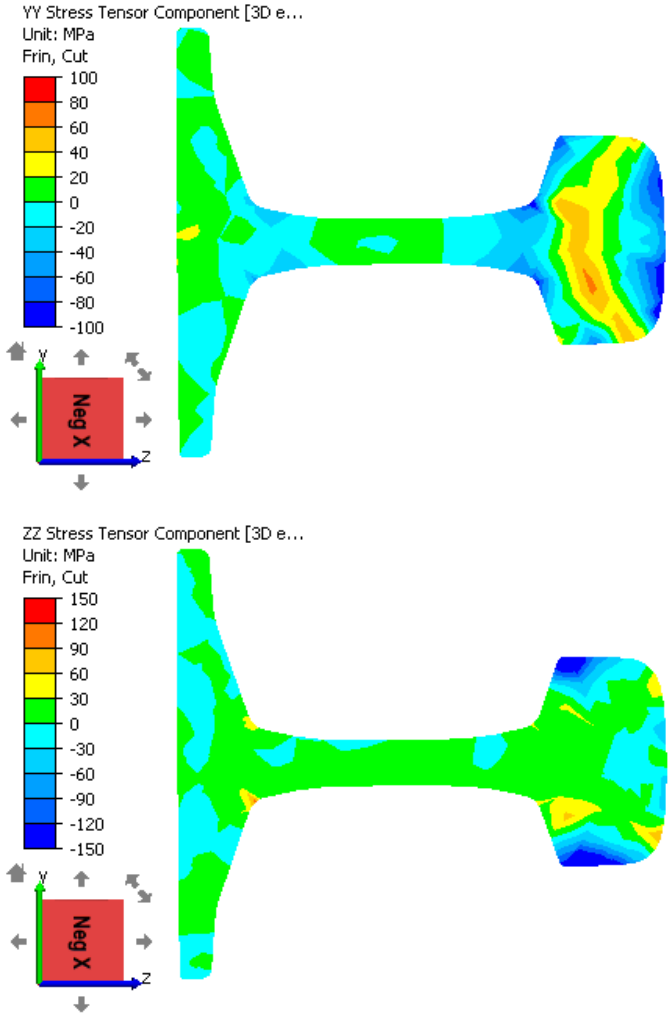

Fig. 11. Distribution of the stress tensor component for straightening simulation (variant 3) after roller 9 after removing the load in the Y-Y and Z-Z plane of the rail

Tables 2 and 3 show the results of the values of residual stresses obtained in the numerical simulation on each roller of the vertical and horizontal straightener for 3 measuring points located on the lower surface of the rail foot – Fig. 12. They illustrate the influence of individual straightener rollers on the stress level; the largest increases of residual stresses in the rail foot are introduced on the R3 and R5 shaft of the vertical straightener. The straightening simulations allowed to determine the impact of changes in the pass design of straightener rollers on the obtained stress level, and at the same time confirmed the correctness of the assumptions made regarding the construction of the rollers.

TABLE 2

The values of residual stresses in the longitudinal direcion for variant 3 in the determined measuring points after individual rolls No. R1 – R7 on a vertical straightener, MPa

Point in the rail	Cross-section behind the roller						
	R 1	R 2	R 3	R 4	R 5	R 6	R 7
1	41	–46	550	20	650	125	73
2	–92	14	–45	35	–20	25	73
3	–84	–7	–88	41	–55	7	49

TABLE 3

The values of residual stresses in the longitudinal direcion for variant 3 in the determined measuring points after individual rolls No. R1 – R9 on a horizontal straightener, MPa

Point in the rail	Cross-section behind the roller								
	R1	R 2	R 3	R 4	R 5	R 6	R 7	R 8	R 9
1	165	118	134	76	286	171	167	68	84
2	99	132	–2	79	–53	–246	–98	4	57
3	–104	–76	–98	–1	–198	21	–32	67	7

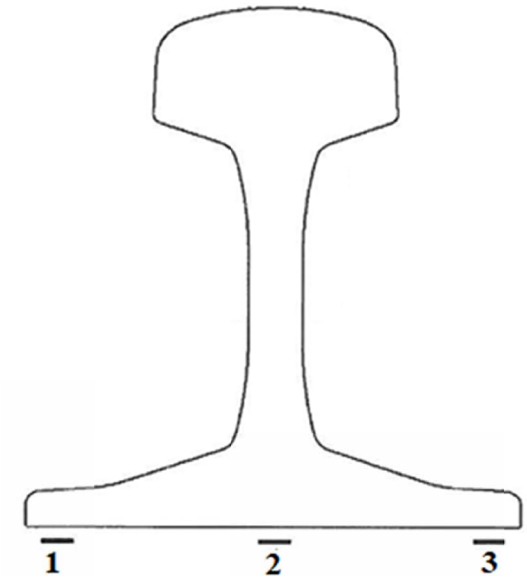

Fig. 12. Location of measuring points

2.5. Residual stress measurement methodology

The basic document that describes the requirements for rails is the European standard EN 13674-1 [2]. It indicates the strain gauge method for assessing the level of stresses in rails as part of product qualification tests. Residual stresses in rails are measured in the centre of the bottom surface of the foot using the cutting method; it consists in sticking a strain gauge on the surface of the tested sample and cutting it near the attached strain gauge. The thickness of the cut out rail slice is 20 mm. As a result of cutting, strains occur in the longitudinal and transverse directions, related to residual stresses. Residual stresses are calculated on the basis of differences between the first and second set of measurement of released strains by multiplying

by the Young's modulus constant. The maximum value of the calculated residual stresses must not exceed 250 MPa. The extension of the EN13674-1 standard requirements is the methodology described in the Technical Conditions of German Railway DBS 918 254-1 [3]. It assumes the measurement of residual stresses in 16 precisely defined locations on the perimeter of the rail in order to assess the symmetry of their distribution and to know their size around the perimeter. The results of the measurements are informative, except for measurements in the foot axis, where the value of residual stresses cannot exceed 250 MPa. In the conducted research, the hole drilling method was also used to determine the state of stress in a small area of impact of working surfaces of profiled rollers. It enables the determination of equivalent uniform principal stresses and their inclination angles with respect to the strain gauge axis, as well as the distribution of these stresses in the 1 mm deep subsurface layer. The measurement methodology is described in ASTM Standard E837-13a [22], and detailed requirements are included in Measurements Group Tech Note TN-503-4.

3. Results and discussion

The results of the numerical simulations were verified in real industrial conditions on the existing production line of a heavy section mill of ArcelorMittal Poland S.A. The experiments were carried out on 120 metres long 60E1 rails made of the R260 steel grade, which were subjected to straightening operations in a set of straighteners with different roller configuration. The studies were carried out in 3 tests, varied by the shape of the working surfaces of straightening rollers. Five rails were straightened in each test, from which a total of 45 samples with a length of 1 metre were taken for the measurement of residual stresses using the strain gauge method. Test sections were always marked in the same three places along the length of each rail, i.e. 4 metres from its end and beginning, and in the middle of the rail. For selected test sections, the distribution of residual stresses on the perimeter of the rail was analysed in 16 measurement locations and in the subsurface layer using hole drilling method. The adopted research plan included the following assumptions regarding the system of straightening rollers:

– the first test used a profiled roller with a smaller concavity on the R3 shaft and a roller with a greater concavity on the R5 shaft of a vertical straightener; the horizontal straightener was configured with the rollers used so far,
– the second test involved the use of rollers with a small flange and without a flange on a horizontal straightener and was carried out in two variants of the vertical straightener installation, i.e. in the first – with a roller with a smaller concavity on the R3 shaft and a roller with a greater concavity on the R5 shaft, and in the second variant rollers from shafts R3 and R5 were swapped,
– the third test also included two variants of one profiled roller installation, i.e. in the first one, one concave roller was used on the R3 shaft, and in the second, this roller was mounted on the R5 shaft; rollers with a small flange and without a flange were used on the horizontal straightener, as in the second test.

The same settings of straighteners and a constant straightening rate of 2.5 m/s were used during each rail straightening experiment, and the rate of rail introduction was 1.0 m/s. The rail temperature during the tests was in the range of 1-8°C. The material for the tests was R260 rail steel grade originating from three different heats, for which a control analysis of the basic elements was performed and the tests of mechanical properties were carried out; the structure of the steel was also checked. The results of these tests are shown in Tables 4 and 5 respectively; there was no significant difference between them, thus allowing the assumption that the material was homogeneous.

TABLE 4

Basic mechanical properties of the tested rails

R260 steel grade	Mechanical properties					
	Tensile strength R_m [MPa]	Yield strength R_{p02} [MPa]	Elongation A_5 [%]	Hardness [HB]	Reduction in area Z [%]	Structure
Test 1	941	579	13,4	av. 289	22	pearlite
Test 2	964	585	12,8	av. 280	21	pearlite
Test 3	973	603	13,8	av. 286	22	pearlite

TABLE 5

Chemical composition

R260 steel grade	Element content in weight [%]					[ppm]
	C	Mn	Si	P	S	H
Test 1	0.72	1.08	0.32	0.012	0.017	1.3
Test 2	0.74	1.07	0.30	0.010	0.015	1.2
Test 3	0.73	1.09	0.32	0.010	0.011	1.2

Figs 13-15 show a graphical presentation of the results of average residual stresses calculated from all measurements taken in the rail foot, on both sides of the web in its neutral axis and in the head, obtained in individual rail straightening tests. Fig. 16 shows the distribution of residual stresses along the entire perimeter of the rails randomly selected from each straightening experiment in accordance with the methodology described in the standard [3], i.e. rail number A505 from the first experiment, rail number A303 determined from the first variant of the second test, and rail A404 selected from the third stage of the research (variant 1). The analysis of the stress distribution on the perimeter of the presented rails reveals their significant differences in the most important measurement points, i.e. the foot and head of the rail in their axis of symmetry and on both sides of the neck in its neutral axis. The A505 and A303 rails show the lowest values of residual stresses in the rail foot with a relatively high level in the rail head, while the A404 rail has a more favorable stress distribution at the main measuring points. The residual stresses for the described tests, recorded in the area from the bottom surface of the rail foot to the lower inclinations of the rail head,

are consistent in type and differ in the values of the results to a small extent. The greatest differences in the symmetry of the residual stress distribution with respect to the vertical axis of rail symmetry for the presented rails are observed on the side inclinations of the rail heads. In the A505 rail this difference amounts to a maximum of 99 MPa, for the A303 rail it was at a much lower level and amounted to 17 MPa, while in the A404 rail the difference in both measuring points was 38 MPa.

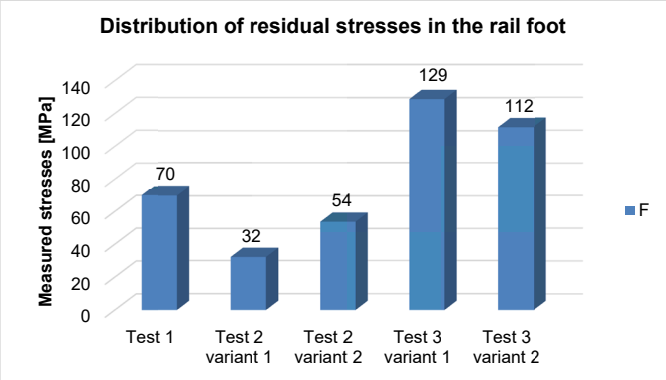

Fig. 13. Distribution of average residual stresses in the rail foot in individual tests

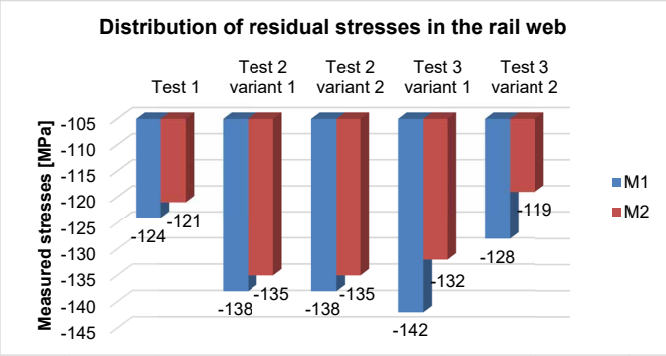

Fig. 14. Distribution of average residual stresses in the rail web in individual tests

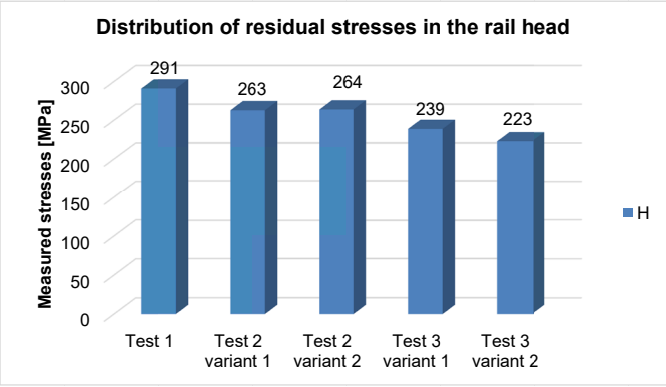

Fig. 15. Distribution of average residual stresses in the rail head in individual tests

Measurements of equivalent uniform residual stresses were also carried out by drilling a hole in the axis of the foot of the

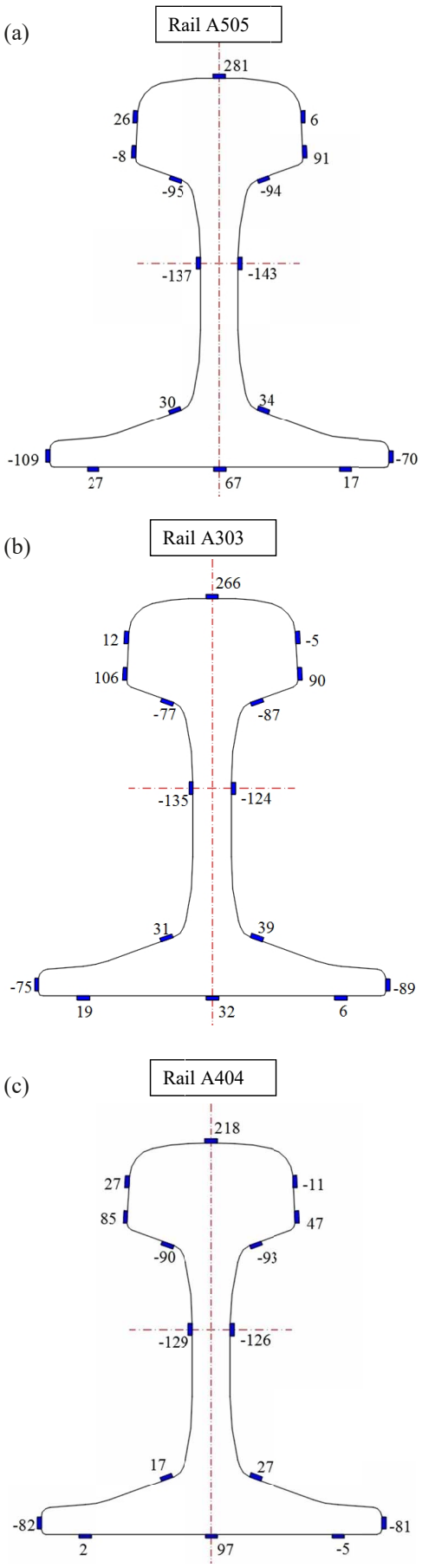

Fig. 16. Distribution of residual stresses [MPa] on the perimeter of rail A505 straightened in the first test, A303 straightened in the second test (variant 1) and A404 straightened in the third test (variant 1)

rail; results of the obtained strains ($\varepsilon 1$, $\varepsilon 2$, $\varepsilon 3$) for the subsequent drilling steps are given in Table 6. The test section originated from straightening test 1. Fig. 17 shows the dependence of the released strains on the hole depth. Table 7 shows the determined components of the state of residual stresses of the tested rail, required by the ASTM E837-13a standard, where:

P – uniform isotropic (equally biaxial) stress,
Q – uniform 45° shear stress,
T – uniform x-y shear stress,
σ_x, σ_y – uniform normal stress in the direction of x and y,
τ_{xy} – uniform shear stress in the x-y plane,
σ_{max} – maximum (more tensile) principal stress,
σ_{min} – minimum (more compressive) principal stress,
β – clockwise angle from the x-axis to the maximum principal stress σ_{max} direction.

TABLE 6

Measured released strains depending on the depth of the drilled hole

Z [mm]	$\varepsilon 1$ [μm/m]	$\varepsilon 2$ [μm/m]	$\varepsilon 3$ [μm/m]
0	0	0	0
0.1	16	17	11
0.2	23	19	9
0.3	33	22	8
0.4	37	24	6
0.5	38	24	–1
0.6	40	22	–5
0.7	43	21	–10
0.8	44	19	–13
0.9	46	17	–17
1.0	46	16	–18

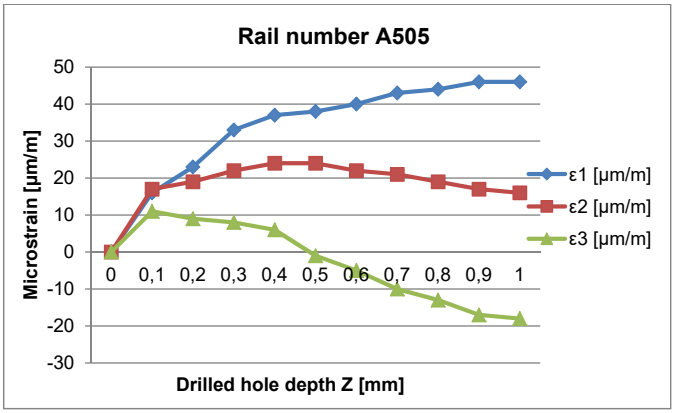

Fig. 17. Dependence of the released strains on the depth of the drilled hole – rail A505

In the hole drilling method, the released strains are measured around the drilled hole from a stress field with a radius of 3 to 4 times greater than R_0, where R_0 – the radius of the drilled hole. For a drill with a diameter of 1.6 mm used for drilling the holes, the diameter of the hole measured with a microscope was 1.9 mm, so the strains were measured from the stress field with a diameter of about 6-8 mm. The determined components of equivalent uniform principal residual stresses are $\sigma_{max} = 15$ MPa and $\sigma_{min} = -64$ MPa, and the angle of inclination β of vector σ_{max} corresponds to 31° and is directed toward the side of the rail with the roller table imprints. Compressive normal stresses $\sigma_x = -47$ MPa in the direction parallel to the axis of the rail have a sign opposite to the measured longitudinal residual stresses in the feet of the rails using the cutting method. This indicates that compressive stresses occur in the small area near the rail axis, while small longitudinal tensile stresses with an average value of 70 MPa recorded in the discussed straightening test number 1 (Fig. 13) dominate in the larger area.

3.1. Summary of results

The analysis of the obtained mean level of residual stresses presented in Figs 13-15 in the first straightening experiment proves that after using the profiled rollers with unchanged settings of the vertical and horizontal straightener and the straightening speed, the tensile stresses in the center of the rail foot symmetry were reduced by more than three and a half times in relation to the level specified in the standard [9]. The compressive state of stresses on both sides of the web was observed in the neutral axis of the rails specified in the experiment, which did not differ significantly in value from the level obtained when straightening the rails with the use of standard straightener rolls. In the rail head, an increase in the mean values of tensile stresses was noticed to the average level of 291 MPa, which proves that the stresses shifted from the rail foot towards the head. In the second straightening test for the variant marked with number 1, the lowest stress level in the rail foot was obtained in all experiments (average value 32 MPa), which is only about 12% of the acceptable standard value [9]. The average level of residual stresses in the rail foot in variant 2 of this test was slightly higher and amounted to 54 MPa, it resulted from a different configuration of the arrangement of the profiled rollers in the vertical straightener. Both the average level of tensile stresses in the rail head and the average value of compressive stresses in both variants of this test were identical. The third straightening test was carried out with one profiled roller in the vertical straightener

TABLE 7

Residual stress components P, Q, T, normal stresses σ_x, σ_y, uniform shear xy-stress τ_{xy}, principal stresses σ_{max}, σ_{min} and clockwise angle β from x-axis to the maximum principal stress direction σ_{max}

Rail number	P [MPa]	Q [MPa]	T [MPa]	σ_x [MPa]	σ_y [MPa]	τ_{xy} [MPa]	σ_{max} [MPa]	σ_{min} [MPa]	β [°]
A505	–25	22	33	–47	–3	33	15	–64	31

and resulted in a favorable stress distribution on the perimeter of the rail, which is expressed by their low level (especially in variant 2) at all measurement points, i.e. in the foot, in the head and web of rail.

A significant decrease in the value of residual stresses measured in the rail foot in relation to the requirements of the standard [2] was observed for all the straightening tests carried out with the use of the new, innovative profiled roller. The lowest residual tensile stress was observed in test 2. Small concavities of the lower surface of the rail foot up to a maximum value of 0.2 mm, probably resulting from the use of double profiled rollers in a tandem arrangement in the vertical straightener, were observed. This phenomenon was not observed in the remaining tests. It should be emphasised that the highest recorded value of mean stresses from all the tests was 129 MPa (test 3, variant 1), which means a reduction of about 32% compared to the average values obtained on rails straightened with standard rollers.

Considering the stress distribution in all rail components, it should be acknowledged that the most favourable outcomes are the results of variant 2 of test 3, where the average level of residual stresses in the rail foot was 112 MPa, with a relatively low level of residual stresses in the rail head of 223 MPa and low values of compressive stresses in the rail web. The optimisation of residual stresses is a desired phenomenon from the point of view of the rail's behaviour in the track. The reduced value of residual stresses in the rail inherited from production has a direct impact on the reduction of the total operational stresses of the rail in the track, and thus affects safety by inhibiting the development of cracks initiated by discontinuities or structural changes in the rail.

Railway rails subjected to straightening experiments passed the acceptance test procedure specified in standard [2] for compliance with the level of mechanical properties, chemical composition, straightness in the vertical and horizontal plane and the tolerance of cross-section parameters. All rails from the discussed tests were thoroughly checked for geometric correctness using legalised acceptance gauges and laser measuring devices.

In order to parametrically estimate the state of stresses in the rail after successive straightening experiments, the average stress was calculated, defined as the standardisation of the complex stress state in the rail to one averaged stress described by formula (4) in accordance with the methodology proposed in the dissertation [23].

$$\sigma_M = \frac{\int_0^{S_E} |\sigma_L| \cdot dS}{\int_0^{S_E} dS} \text{ [MPa]} \tag{4}$$

where:

σ_M – averaged stress,
σ_L – longitudinal stress,
S_E – orthogonal surface.

The theoretical cross-sectional surface of the 60E1 rail nominal amounting to 76.70 cm^2 was adopted for the calculations, the rail surface was divided into 16 measurement fields corresponding to the locations where the residual stresses were measured (Fig. 18) and the surface of each of these areas was calculated – Table 8. The determined values of averaged stress are shown in Table 9. The concentration of stress measurements up to 16 points on the perimeter and the associated division into smaller areas of the rail surface gives an accurate image of the complex state of residual stresses in the rail, which can be represented by calculated averaged stress. For the purposes of comparison, the averaged stress for the selected rail straight-

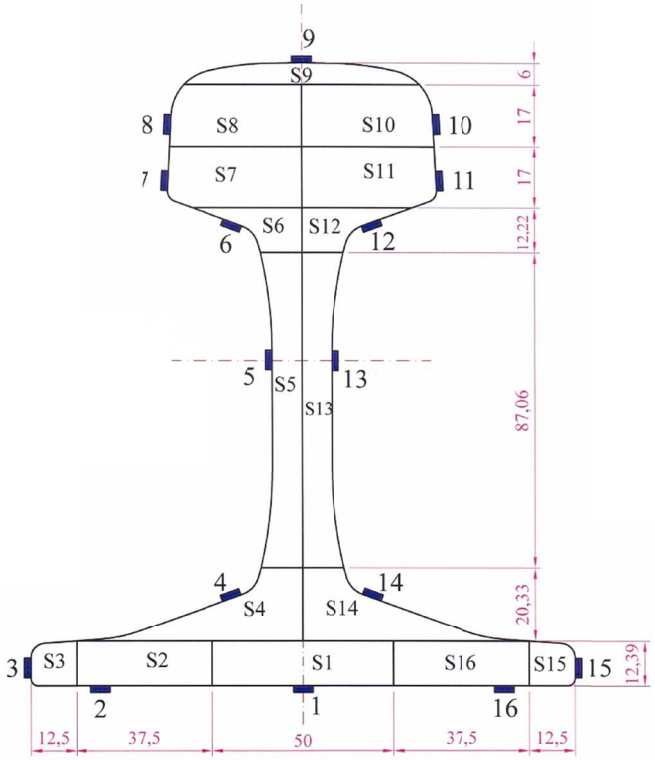

Fig. 18. Division of measurement areas in rail 60E1 for 16 measuring points for residual stresses on the rail perimeter, source [23]

TABLE 8

Surface areas for measurement areas from Fig. 16, source [23]

Area	Surface area [mm^2]
S1	619.64
S2	464.71
S3	145.56
S4	551.97
S5	776.62
S6	210.7
S7	616.85
S8	604.04
S9	309.45
S10	604.04
S11	616.85
S12	210.71
S13	776.62
S14	551.97
S15	145.56
S16	464.71

TABLE 9

Calculated values of averaged stresses of rails in individual tests

Reference measurement [MPa]	Test 1 [MPa]	Test 2 variant 1 [MPa]	Test 2 variant 2 [MPa]	Test 3 variant 1 [MPa]	Test 3 variant 2 [MPa]
99	71	71	75	81	68

ened using the existing technology was calculated. Each of the straightening tests was characterised by a much lower calculated value of averaged stress σ_M in relation to the reference measurement. The reference measurement was determined on the basis of testing the distribution of residual stresses on the perimeter of the straightened rail using the so far used technology of straightening with traditional rollers.

The largest 31% decrease of σ_M was obtained for variant 2 of test 3. Such a significant reduction of the averaged stress proves the optimisation of the residual stress distribution on the perimeter of the rail; it is also reflected in the tensometric measurements of stresses in this test, where not only tensile stresses in the foot of the rail decreased, but their decrease was also observed in the rail head, which is a preferred phenomenon.

Linking the value of residual stresses in the rail foot and head with the averaged stress of the rail calculated using formula (4) allows for a comprehensive assessment of the impact of the applied variant of the straightener roller system, and for a determination of the impact of changes in the roller pass design on the state of residual stress in the rail and geometrical correctness of the finished product. Such a holistic approach provides a tool to verify the applied rail straightening model not only in terms of the level of residual stresses introduced in the measuring point, required by the EN13674-1 standard, located in the centre of the rail foot symmetry, but also allows to assess the stress distribution over the entire rail cross-section and to estimate the rail's averaged stress, which should be taken as an efficiency index of reduction of residual stresses in the rail. The method is of technological significance and is useful for the evaluation of the operational behaviour of rails in the tracks. It can be assumed that the lower the value of the calculated averaged stress, the less prone the rail will be to permanent deformation and loss of cohesion, and therefore it will directly translate into the safety of railway traffic, where the rail is the most important element of the track.

4. Conclusions

The works on optimisation of residual stresses in rails presented in this article are part of an important and current research area related to the development of railway infrastructure and increasing its operational reliability and safety of railway transport. The state of stress in rails is a complex phenomenon, characterised by multiple conditions that affect different stages of rail production. First of all, it depends on the curvature of the rail before the straightening process and the bending settings used during it on individual shafts of straightening machines; the construction of the straightening rollers also has a significant influence. The state of residual stress inherited from all technological operations translates directly into the operational properties of the rails.

Numerical simulations, industrial experiments in a set of straighteners and laboratory tests contributed to the extension of knowledge in the field of the influence of the shape of straightener rollers on the value of residual stresses in the rails. The evaluation of the effects of each straightening experiment using re-calibrated rollers included the analysis of the applied stresses after straightening, their distribution on the rail cross-section, averaged stress and parameters of the cross-sectional and straightness tolerances in relation to the requirements of the standard as superior values.

The performed tests of residual stresses distribution in the rail foot by the hole drilling method in straightening tests show that in a small area near the rail axis there are slight compressive or low tensile residual stresses in the direction parallel to the rail axis; the level of these stresses is much lower in relation to the released stresses measured from the entire volume of the foot in the rail slice cutting test according to the EN13674-1 standard. It allows concluding that the use of profiled rollers changes the value of residual stresses in the area of their contact with the rail material. Therefore, it is correct to conclude that it is possible to control the state of stress in a targeted manner by modifying the calibration of straightener rollers.

Acknowledgements

This study was supported by the National Centre for Research and Development, Poland, under the research project entitled "Innovative and safe rails with a low level of residual stresses in the foot of the rail" – POIR.01.02.00-00-0167/16.

REFERENCES

[1] S. Żak, J. Sarna, J. Merta. Ocena jakości szyn produkcji Huty Katowice, Materiały XII Konferencji Naukowo-Technicznej Drogi Kolejowe, 409-426 (2003).

[2] European Standard EN 13674-1:2011+A1:2017 Railway applications – Track – Rail. Part 1: Vignole railway rails 46 kg/m and above, (2011).

[3] Technical Conditions of German Railway DBS 918 254-1 – Rail. Part 1: Vignole railway rails 46 kg/m and above, (2019).

[4] Indian Standard IRST-12-2009 Indian Railway Standard Specification for flat bottom rails, (2009).

[5] National Standard of the Russian Federation GOST R51685 Railway rails – General Technical Conditions, (2013).

[6] AREMA Standard – American Railway Engineering and Maintenance-of-Way Association. Chapter 4 Rail, Part 2 Manufacture of Rail, (2016).

[7] W. Guericke, J. Weiser, H. Schmedders, R. Dannenberg, Ursachen von Schienen-Eigenspannungen infolge Rollenrichtens und Beitrag zur Verringerung, ETR Eisenbahntechnische Rundschau, DK 625.143:539.4.014.13:625.143.001.5, **7-8** (1995)

[8] https://tvnwarszawa.tvn24.pl/informacje,news,czy-tory-byly-zlebrfalujace-szyny-w-ursusie,257960.html

[9] https://alchetron.com/Hatfield-rail-crash

[10] E. Jericho, M. Weiße, Beitrag der Eigenspannungen zum Gebrauchsverhalten von Schienen, Internationales Symposium „Schienenfehler", Brandenburg an der Havel, **10-1** ÷ **10-9** (2000).

[11] W. Guericke, W. Heller, J. Kasprowicz, M. Weiße, Verbesserte Bruchsicherheit von Schienen durch optimiertes Rollenrichten, ETR Eisenbahntechnische Rundschau **50** Nr. 9, 541-551 (2001).

[12] H. Song, P. Wang, L. Fu, M. Chen, Z. Wang, H. Sun, Straightening regulation optimization on the residual stress induced by the compound roll straightening in the heavy rail, Shock and Vib. **18**, 171-180 (2011). DOI: https://doi.org/10.3233/SAV20100599

[13] G. Finstermann, F. Fiscger, G. Shan, G. Schleinzer, Residual stresses in rails due to roll straightening, Steel Res. **7**, 272-278 (1998). DOI: https://doi.org/10.1002/SRIN.199805549

[14] W. Guericke, J. Weiser , H. Schmedders, R. Dannenberg, Ursachen von Schienen-Eigenspannungen infolge Rollenrichtens und Beitrag zur Verringerung, ETR Eisenbahntechnische Rundschau **46** 10, 655-662 (1997). DK 625.143:539.4.014.13:625.143.001.5

[51] E. Jericho, Schienen mit geringeren Eigenspannungen, ETR - Eisenbahntechnische Rundschau **46** Nr. 10, 663-666 (1997). DK 625.143:539.4.014.13.002.234

[16] M. Pazdanowski, Residual Stress development in railroad rails – a parametric study, Technical Transactions – Civil Engineering **6-B**, 83-94 (2014).
DOI: https://doi.org/10.4467/2353737XCT.14.382.3693

[17] M. Pazdanowski, Residual stresses as a factor of railroad rails fatigue, Technical Transactions – Civil Engineering **4-B**, 39-46 (2014).

[18] M. Pietrzyk, R. Kuziak, Numerical simulation of controlled cooling of rails as a tool for optimal design of this process, Computer Methods in Materials Science **12**, 4, 233-243 (2012).

[19] S. Żak, W. Woźniak, V. Pidvysots'kyy, R. Mariusz, Wpływ kształtu powierzchni roboczej rolek prostujących prostownicy pionowej na poziom naprężeń własnych w szynie kolejowej, Hutnik – Wiadomości Hutnicze **86**, 10, 319-323 (2019).
DOI: https://doi.org/10.15199/24.2019.10.4

[20] S. Żak, D. Woźniak, V. Pidvysots'kyy, T. Urbanik, The influence of the shape of working surface of straightening rollers of vertical and horizontal straightening machines on the state of residual stresses in railway rail – second stage of researches, Journal of Metallic Materials **72**, 1, 48-58 (2020).
DOI: https://doi.org/10.32730/imz.2657-747.20.1.4

[21] S. Żak, D. Woźniak, V. Pidvysots'kyy, T. Dzierżawczyk, Wpływ kształtu powierzchni roboczej rolek prostujących prostownic pionowej i poziomej na stan naprężeń własnych w szynie kolejowej – etap trzeci badań, Hutnik – Wiadomości Hutnicze **87**, 9, 225-232 (2020). DOI: https://doi.org/10.15199/24.2020.9.3

[22] ASTM E837-13a Standard – Standard Test Method for Determining Residual Stresses by the Hole-Drilling Strain-Gage Method, (2013).

[23] S. Żak, PhD thesis, The way of controlling the state of residual stresses in railway rails by modifying the roll pass design of rolls and straightening rollers, Silesian University of Technology Poland, (2019).